JOURNAL OF MATERIALS SCIENCE 13 (1978) 2541–2547

Thermal polycondensation of ammonium paratungstate, $(NH_4)_{10}[W_{12}O_{40}(OH)_2].4H_2O$

A. B. KISS*, T. NEMETH, E. SZALANCZY*
Research Institute for Technical Physics of the Hungarian Academy of Sciences, Budapest, Hungary

Connected with the examination of the thermal polycondensation of ammonium paratungstate pentahydrate the chemical and morphological properties of intermediate phases formed during the thermal decomposition of APT have been investigated. We have studied the pH and the turbidity of the aqueous solutions of the intermediate phases, the solubility of the phases, and their rehydratation capability as well as the morphology of the crystallite granules and the grain size distribution. These properties of the original APT have been related to the same properties of the products of decomposition formed between different temperature ranges. The results obtained show unambiguously that each of the above mentioned properties suddenly changes in the temperature range 225 to 250° C. This temperature range coincides with the formation temperature of a new phase called APT II. The most probable formula of APT II is $(NH_4)_8[H_2W_{13}O_{43}(OH)_2]\cdot H_2O$.

1. Introduction

Throughout the world tungsten incandescent bodies suitable as light sources are produced from ammonium paratungstate (APT) as the starting material. Particular importance is therefore attached to research aimed at the fundamental understanding of the thermal behaviour of this complex polymeric compound. The process of thermal decomposition has previously been investigated by a number of authors with thermoanalytical methods [1–5], while we have studied the process by thermal analysis and infra-red spectrometry [6, 7] and other supplementary methods [8–10]. In the course of the work we acquired much new knowledge, but our results at that time left open various possibilities for the interpretation of some of the findings. In the present paper we wish to contribute to the detailed clarification of some questions via further supplementary examinations.

2. Experimental methods and results

Some properties of intermediate phases formed during the thermal decomposition of APT have been investigated in connection with the results of earlier thermoanalytical studies [1–10]. In all experiments APT samples with identical characteristics were used in order to avoid possible effects arising from differences in composition, structure, morphology and grain size.

2.1. pH measurements

Intermediate phases were prepared in 400 mg portions by interruption of the reaction at various temperatures in a thermobalance furnace, heated at a rate of 150° C h^{-1}. From these, 2 g portions were taken in 100 ml distilled water and the pHs of the solutions were measured after stirring for 2 h. Such a long time was necessary because of the low rates of dissolution of APT and the intermediates. The pH values were measured with a Radelkisz OP-205 precision pH meter and an OP 8011/A combined glass electrode. pH values of aqueous solutions of intermediate phases formed at various temperatures are shown in Fig. 1.

2.2. Solubility examinations

From the materials prepared as above, 2 g portions

*Research Institute, United Incandescent Lamp and Electricity Co., Budapest, Hungary.

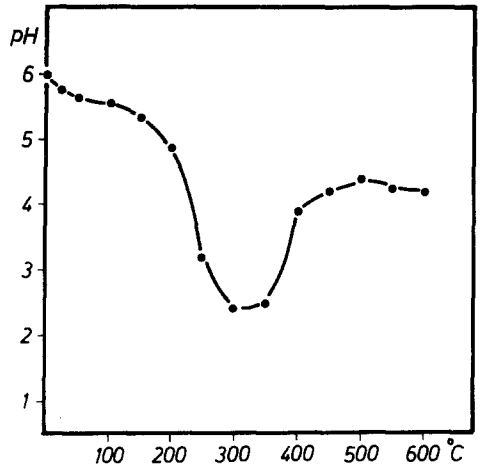

Figure 1 pHs of aqueous solutions of intermediate phases formed at various temperatures .

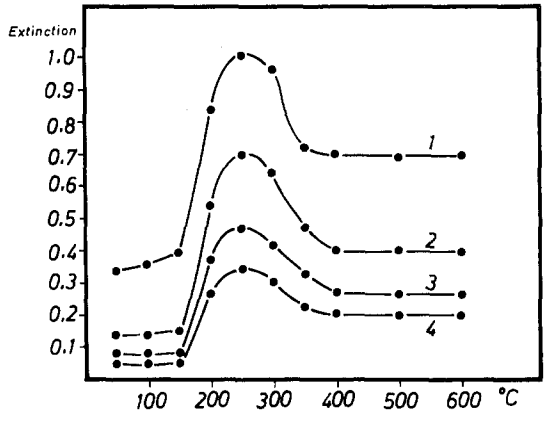

Figure 3 Extinction values characteristic of turbidities of solutions of intermediate phases formed at various temperatures after a sedimentation time of (1) 1 min, (2) 5 min, (3) 10 min, (4) 20 min. Layer thickness: 1 cm; Wavelength: 600 nm.

were mixed with 50 ml water, and 24 h later the concentrations of the saturated solutions were measured. Aliquots were taken, the solution was evaporated to dryness, the residue was annealed at 700° C for 1 h, and the dissolved APT was measured as WO_3. Fig 2 gives the solubilities of intermediate phases formed at various temperatures.

2.3. Turbidity measurements

150 mg portions were mixed with 10 ml glycerol–ethanol (2:1), the mixture was thoroughly shaken, a sample was taken in a 1 cm cell, and the rate of change of turbidity measured at 600 nm. Fig. 3 illustrates the relationship between the turbidity

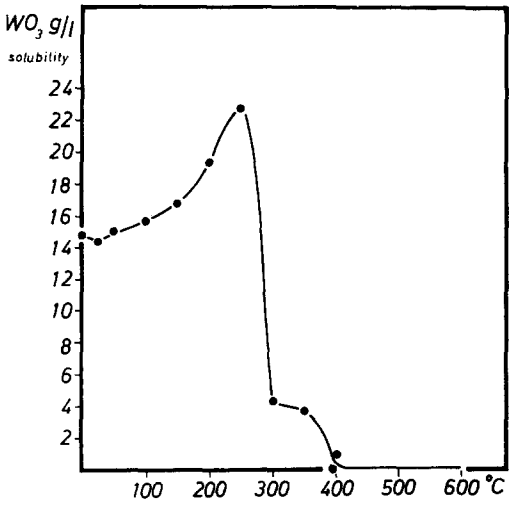

Figure 2 Solubilities of intermediate phases formed at various temperatures.

values measured after the passage of various stages and the formation temperatures of the intermediate phases.

2.4. Rehydration examinations

400 mg material was uniformly spread in a thickness of approximately 1 mm in a flat crucible with a diameter of 22 mm. The rehydration rate was measured in a closed system in an atmosphere with a partial pressure $p_{H_2O} = 12$ mm Hg (1600 Pa) after interruption at various temperatures during heating at a rate of 150° C h^{-1}. The NH_3 and WO_3 contents of the samples were determined after completion of the rehydration; the compositions calculated for 12 WO_3 are given in Table I. Curve (a) of Fig. 4 shows the H_2O content per 1 WO_3 in the rehydrated phases, and curve (b) the earlier measured H_2O/WO_3 values [9–11] obtained when the heat-treated phases were stored in a P_2O_5 desiccator prior to examination.

2.5. Morphological study of crystallite grains and grain sizes

The morphology of the crystallite grains was studied on a Stereoscan 600 scanning electron microscope. The heat treatments were carried out either in air or in 30% H_2 + 70% N_2, with heating rates in the range 50 to 1000° C min^{-1}. The variation in the grain size distribution was evaluated on the basis of scanning electron micrographs and the results obtained with a sedimentation balance. In the latter case the effects of the geometric factors influencing the sedimentation rate were neglected, and hence information was obtained only on the

TABLE I Chemical compositions of rehydrated phases

Temperature (° C)	NH_3 (%)	WO_3 (%)	H_2O (%)	$(NH_4)_2O$ (mol)	WO_3 (mol)	H_2O (mol)	H_2O/WO_3
20	5.45	88.73	5.84	5.00	12	5.00	0.416
100	5.45	89.0	5.55	5.00	12	4.63	0.386
150	5.36	89.0	5.64	4.93	12	4.87	0.405
200	4.39	89.0	6.61	4.03	12	7.45	0.620
225	4.10	89.2	6.70	3.76	12	7.85	0.654
250	3.50	90.5	6.00	3.15	12	7.09	0.590
300	1.55	97.5	0.95	1.30	12	0.204	0.017
350	1.00	98.5	0.50	0.83	12	–	–
400	0.35	99.4	0.25	0.57	12	0.99	0.082
500	0.00	100.0	0.00	–	12	–	–

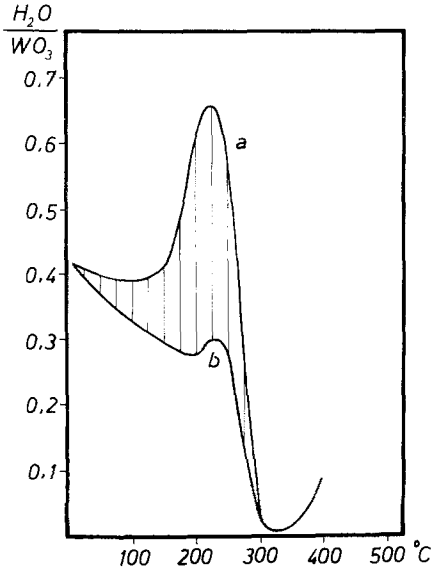

Figure 4 Rehydration capacities of the intermediate phases (a) H_2O content per 1 WO_3 in the rehydrated phases; (b) H_2O content per 1 WO_3 in phases maintained above P_2O_5 following preparation.

relative grain size distribution. The sedimentation was carried out with 0.5 g samples suspended in 250 ml ethylene glycol in a sedimentation balance thermostated at 25° C. The relative grain size distribution (wt %), and the scanning electron micrographs of APT samples heat-treated in air are given in Table II and Fig. 5.

3. Discussion

3.1. Thermal decompositon

The interpretation of the new experimental data requires a short reference to the results of earlier thermoanalytical studies [6–11], in which we report thermoanalytical curves for APT, measured with the thermogravimetric and infra-red spectrophotometric method; the essence of these is that the concentration changes of the gaseous products formed in the course of the thermal process were recorded and measured continuously by infra-red spectrophotometry (Fig. 6).

On the basis of Fig. 6, with the aid of the previously elaborated calculation methods [6, 7], the data listed in Table III were obtained on the compositions of the intermediate phases formed in the individual steps.

It can be seen that five reaction stages can be distinguished up to the transformation to WO_3.

3.2. Supplementary chemical experimental results

The pH values arising as a result of dissolution of the intermediate phases display a minimum in the range of the ammonium–bronze phases formation at 300° C (Fig. 1). The strong pH decrease beween 150 and 250° C is in agreement with the experimental results presented in Fig. 6, for dry

TABLE II Relative grain distribution (wt %) of APT samples heat-treated in air

Temperature of heat treatment (° C)	*d* nominal (μm)				
	20	20–40	40–70	70–110	110
150	5.1	17.9	35.4	27.9	13.7
200	8.6	25.3	35.0	18.5	12.6
250	13.3	33.4	25.3	12.1	5.9
300	5.4	26.2	35.0	26.8	6.6
350	5.5	26.4	37.0	24.0	7.1
400	5.6	25.3	39.0	23.2	6.9
600	31.1	37.2	14.7	16.2	0.8

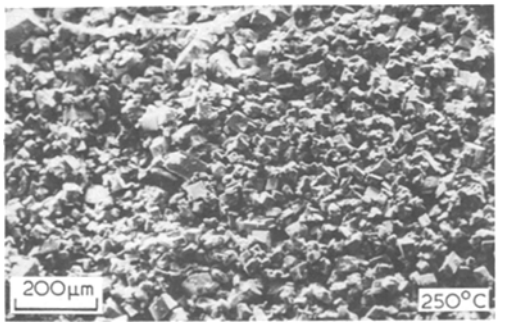

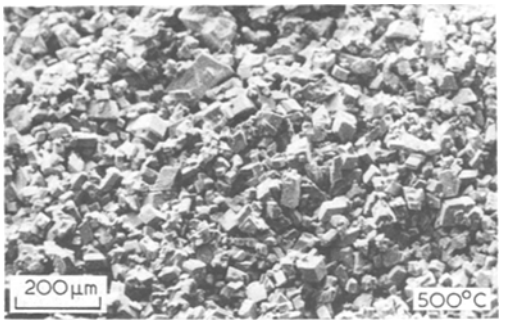

Figure 5 Scanning electron microscope photos of APT samples heat-treated in air.

NH_3 gas is lost from the system in this temperature, range as a consequence of the thermal splitting of the NH_4^+ ions.

If the polytungstate formed in step III is prepared in infra-red spectrophotometric purity and is mixed with the initial paratungstate crystals in an increasing percentage, and if the mixture is then dissolved under the same conditions as above,

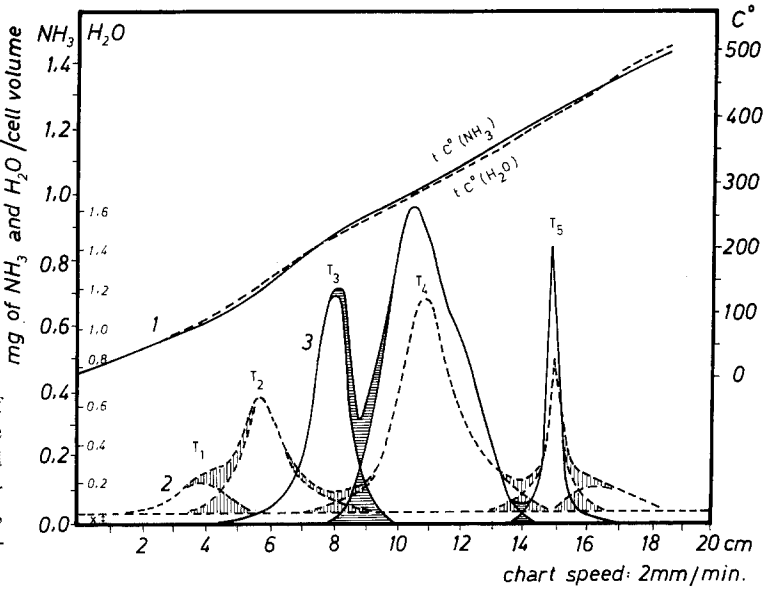

Figure 6 The concentration changes of the gaseous products formed in the course of the thermal process, recorded continuously by infra-red spectrophotometry. (1) Heating rate, (2) H_2O curve, (3) NH_2 curve, (x) Equilibrium moisture content of the carrier gas.

TABLE III Chemical compositions of intermediate phases formed in the various temperature intervals, prior to rehydration

TG steps i.r. maxima	Temperature	$(NH_4)_2O$	WO_3	H_2O	Calculated molecular weight per 1 WO_3
Tungsram basic material	20	5.0	12	5.0	261.1
I	20–130	5.0	12	4.0	259.6
II	70–170	5.0	12	2.0	256.6
III	100–280	3.75	12	3.25	253.1
IV	190–390	0.67	12	0.83	236.0
V	340–480	–	WO_3	–	231.9

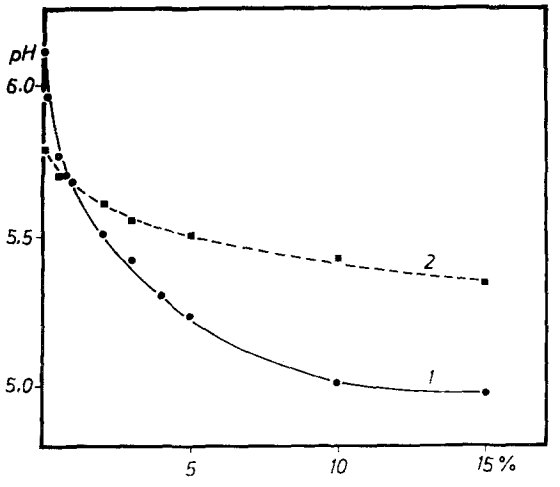

Figure 7 pH change of aqueous solutions of APT as a function of the percentage amount of intermediate formed in step III (between 225 and 250° C).

the pH dependence depicted in Fig. 7 is obtained. It is clear that the presence of even 0.1% of the intermediate phase can be detected, which in practice allows the detection of possible over-drying of the APT by means of pH measurements.

The rate of dissolution of the intermediate phases similarly exhibits a maximum for the phase produced in step III, i.e. at 225 to 250° C (Fig. 2). The curves of Fig. 3 clearly indicate that the maximum in the dissolution rate in Fig. 2 may be connected not only with the chemical nature of the compounds, but also with grain size or morphology changes occurring during the development of the intermediate phases, since the turbidity values measured after the passage of various intervals also result in maximum curves of a similar nature.

It is striking that the amount of H_2O rehydrated per 1 WO_3 similarly exhibits a maximum for the intermediate formed between 225 and 250° C [Fig. 4, curve (a)]. The maximum at around 225° C in curve (b) arises from the fact that dry NH_3 gas leaves the crystal lattice at this temperature and, in accordance with the composition of the $(NH_4)_2O$ group, 1 mole of H_2O must remain in the crystallite grains after the departure of 2 moles of NH_3 [9]. From Table III too it emerges that the H_2O content of this phase does indeed increase at this point.

3.3. Morphological study of crystallites

A number of authors have investigated the morphologies of the APTs and the structural and morphological changes occurring during their thermal decompositions [2, 12–14]. In these papers the emphasis is placed on the study of the higher-temperature range, and the connection between the external morphological characteristics of the initial APT and the WO_3s formed at the different temperatures is examined in detail [12, 14]. Thus, no mention is made at all of the phase with modified structure which always appears at between 200 and 250° C during the thermal polycondensation, nor of the range of the tungsten-bronzes, which both play an important role in the technological reduction process. No matter how the decomposition of the APT to WO_3 is carried out (continuous heating, or continuous heating and isothermal heat-treatment), the system always goes beyond the intermediate phases found in [9–11]. A deeper insight into the overall process is obtained, therefore, if the crystal structural and morphological states occurring at the intermediate temperatures are inserted between the characteristics of the APT and the WO_3.

Similarly to the above anomalies, the grain sizes of APT samples heat-treated in air exhibit an extreme distribution at around 250° C. According to sedimentation measurements too (Table II), the average grain size of the samples gradually decreases up to 250° C; then with further increase of the temperature the average grain size increases slowly, until at around 500° C there is again an intensive diminution. Unexpectedly, it was found that variation of the heating rate did not affect the distribution of the grain size fractions given in Table II to a significant extent. The photos in Fig. 5 reveal the temperature-dependent characteristic change of the grain size of the heat-treated samples; this shows up most markedly in the strong grain size diminution at about 250° C.

The low-temperature diminution can be attributed to the fissures accompanying the departure of the H_2O and NH_3 contents with the development of a more porous and looser morphological structure. This process makes its effect felt more strongly in the morphology in step III.

3.4. Structural argumentation

According to the earlier published infra-red spectrum and X-ray diffraction photos, in step III, between the temperature values of 200 and 250° C, the structure of the APT is modified, as shown by changes in the diffraction *d* values, the infra-red absorption wavenumbers and the cell parameters

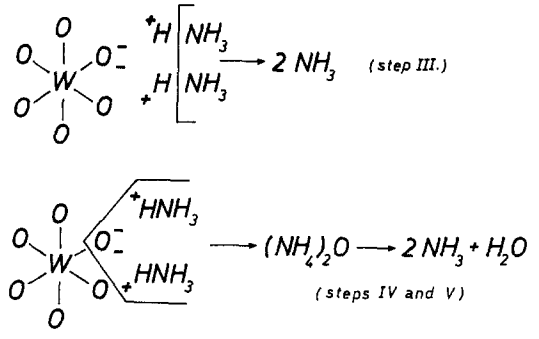

Figure 8 Schematic illustration of processes accompanied by departure of NH_3 gas, from a crystallographic aspect.

[9]. As can be seen in Fig. 6, the NH_3 gas may leave the crystal either in the dry form (step III) or together with water vapour in accordance with the composition of the $(NH_4)_2O$ group (steps IV and V). The conditions illustrating these two processes are simplified in the scheme of Fig. 8, without assuming that the NH_4^+ ions are ascribed to strictly localized, particular oxygen atoms in the crystal lattice of the APT.

Accordingly, in the outer coordination sphere of the paratungstate ion different chemical bonding and energetic conditions of the $W-O^- \ldots NH_4^+$ groups have to be assumed, such that the effect of the heat treatment results in the thermal breakdown of the NH_4^+ ions in the one case, and in the splitting-off of $(NH_4)_2O$ groups together with an oxygen atom from the lattice structure in the other case.

The question was raised earlier of whether the hydrogen atoms remaining after the thermal decomposition of the NH_4^+ ions are H^+ ions with an acidic character, or whether they form W–OH groups bound by covalent forces. On the basis of our earlier results [9, 10] we finally came to the conclusion that the most probable formula for the phase formed in step III is: $(NH_4)_8[W_{13}O_{41}(OH)_4] \cdot H_2O$.

However, this structure does not explain why a substantially lower pH is obtained on dissolution of the compound, in comparison with a value pH = 6 for the solution of the starting APT. It is beyond doubt that very involved complex equilibrium conditions can develop in solution on the interaction of the paratungstates and the intermediates with water, but it would exceed the scope of the present paper to take these into account here. To a first approximation, however, the findings would be easily interpretable if it is assumed that dissociable acidic H^+ ions remain on the WO_6 octahedra of the paracrystal on the departure of the NH_3 gas. Since the starting paratungstate contains 2 moles of structural OH groups bound by covalent forces [9, 10], which will certainly still be stable at the temperature (225 to 250° C) of formation of the intermediate in question, doubt cannot be cast on the earlier infra-red spectrophotometric results according to which the intermediate step III phase also possesses these OH groups. We find agreement between the present pH measurement data and our earlier experimental results, therefore, if it is assumed that both the structural OH groups bound by covalent forces (W–OH) and the dissociable H^+ ions ($W-O^- \ldots H^+$) are present simultaneously in this phase. Taking these circumstances into account, we can give the most probable formula for the intermediate phase as $(NH_4)_8[H_2W_{13}O_{43}(OH)_2] \cdot H_2O$.

To decide whether this phase should be classified among the para- or the metatungstates, let us consider the following composition quotients as one of the criteria of classification.

	paratungstate	intermediate	metatungstate
$\frac{WO_3}{M_2O}$	$\frac{12}{5} = 2.4$	$\frac{13}{5} = 2.6$	$\frac{12}{3} = 4.0$

where M may be any monovalent cation: NH_4^+, K^+, Na^+ or H^+.

On the basis of this criterion, the intermediate in question must be regarded as a paratungstate variant. This follows not only from its composition, but also from the fact that the structure of the infra-red spectrum of the phase and its X-ray diffraction line system are fairly close to those of the starting paratungstate, although they can be well differentiated from these [9–11]. At the same time, the infra-red spectrum of the phase differs decisively from the spectrum of metatungstate [15].

In the interest of differentiation, we propose that in the future the basic compound, $(NH_4)_{10}[W_{12}O_{40}(OH)_2] \cdot 4H_2O$, should be named paratungstate I, and the variant formed from this by heat-treatment at around 225° C, $(NH_4)_8[H_2W_{13}O_{43}(OH)_2] \cdot H_2O$, should be named paratungstate II.

4. Conclusions

As regards the overall thermal process, the interval between 225 and 250° C is a distinctive one not

only because of the appearance of the paratungstate II phase, but also because numerous changes in properties coincide here, or rather they are connected with the formation of this phase. At this point there is a very great increase in the solubility of the substance; apart from the changes in chemical character and grain size, this may also be correlated with an increased tendency to rehydration. Simultaneously with the appearance of the paratungstate II, a grain diminution occurs during the thermal decomposition. This finding is of importance, for thereby in the subsequent reduction process the substance may possess morphological properties which play a determining role in the powder-metallurgical production of tungsten bars with favourable structure. The characteristics anomaly of the presented grain size distribution probably also appears in the grain size distribution of powder-metallurgical W metal powder.

References

1. J. NEUGEBAUER, J. A. HEGEDUS and T MILLNER, *Z. anorg. allg. Chem.* **302** (1959) 50.
2. Y. AHN, *J. Japan Soc. Powder Metallurgy* 8 (1961) 253.
3. W. WANEK, *Silikaty* **6** (1962) 70.
4. G. KOHLSTRUNG, *Phys. Stat. Sol.* **2** (1962) 85.
5. H. HENKES, *ibid.* **9k** (1965) 105.
6. B. A. KISS, *Acta Chim. Acad. Sci. Hung.* **61** (1969) 207.
7. *Idem, ibid.* **63** (1970) 243.
8. B. A. KISS, G. BEREND and P. GADO, 3rd Anal. Conference Budapest (1970) p. 311.
9. B. A. KISS, P. GADO, and J. A. HEGEDUS, *Acta Chim. Acad. Sci. Hung.* 78 (1972) 30.
10. B. A. KISS and L. CHUDIK-MAJOR, *ibid.* 78 (1973) 237.
11. B. A. KISS, (in Hungarian) Dissertation, Hungarian Academy of Sciences (1973).
12. A. YAMAMOTO, *Nippon Tungsten Review* 7 (1974) 1.
13. A. K. BASU and F. R. SALE, *J. Mater. Sci.* **10** (1975) 571.
14. *Idem, ibid.* **12** (1977) 1115.
15. O. GLEMSER, W. HOLZNAGEL, W. HÖLTJE and E. SCHWARZMANN, *Naturforsch.* **20b** (1965) 725.

Recieved 4 January and accepted 15 May 1978.